EMC-ORIENTED ANALYSIS OF ELECTRIC NEAR-FIELD IN HIGH FREQUENCY

Ali Alaeldine, Olivier Maurice, Jérome Cordi, Richard Perdriau, Mohamed Ramdani

EMC-ORIENTED ANALYSIS OF ELECTRIC NEAR-FIELD IN HIGH FREQUENCY

Ali Alaeldine[12], **Olivier Maurice**[3⋆], **Jérôme Cordi**[124], **Richard Perdriau**[1], and **Mohamed Ramdani**[1]

[1] ESEO - 4, rue Merlet-de-la-Boulaye - BP 30926 - 49009 Angers Cedex 01 - France
[2] IETR - INSA de Rennes - 20, avenue des Buttes de Coësmes - 35043 Rennes Cedex - France
[3] EMC for Automotive Systems Group - Research and Development Center - PSA (Peugeot Citroën) - Route de Gizy - 78943 Vélizy-Villacoublay Cedex - France
[4] ATMEL Nantes - La Chantrerie - Route de Gachet - 44300 Nantes - France

Abstract. This paper introduces an EMC-oriented study of the frequency-domain behavior of the electric field generated by two dipole antennas. First of all, the theoretical expression of this field is analyzed and confronted with the macromodel commonly used in electrical circuits. Then, the most significant components of the expression are included into the topological study of a two-dipole network through Kron's method. Finally, computed results are compared with experimental ones and show significant similarities.

Keywords - EMC, near field, dipole, Kron, equivalent circuit.

1 INTRODUCTION

Common EMC-targeted equivalent macromodels of electric near field interaction are generally based on the use of a capacitance which translates Poisson's potential-related equation into a current-related equation. In very high frequency, a far field interaction is added to the electrostatic one [1] [2]. However, taking into account both effects at the same time is a difficult task. In fact, in classical SPICE-based electric simulators, this far field interaction must be coded using mathematical equations, which are not easy to use in this case. Moreover, 3D simulation methods are scarcely compliant with both near and far field requirements, thus preventing accurate modeling.
Therefore, this paper introduces a new approach, based on a study of the global behavior of the electric field generated by two dipole antennas, and which automates the re-use of 3D computations while keeping the same accuracy as the one obtained through analytical fitting. It is based on the results obtained in a previous paper [3].

2 THE ELEMENTARY CURRENT MODEL

On one hand, an elementary model of the electrical field generated by an elementary dipole is given in Eq. 1 [4] :

$$\overrightarrow{E} = \frac{-p_0}{4\pi\varepsilon_0 r \lambda\!\!\!^{-2}} \left\{ \left[-1 + \left(-2\frac{\lambda\!\!\!^{-2}}{r^2} - 2\jmath\frac{\lambda\!\!\!^{-}}{r} + 1 \right) \right] \cos\theta \, \overrightarrow{r_1} \right.$$

⋆ Corresponding author - E-mail : olivier.maurice6@wanadoo.fr

$$+\left[1+\left(\frac{-\lambda^2}{r^2}-\jmath\frac{\lambda}{r}\right)\right]\sin\theta\ \overrightarrow{\theta_1}\Bigg\}\ e^{\jmath\omega t} \tag{1}$$

in which p_0 is the electrical moment, λ the wavelength divided by 2π, r the distance between the center of the moment and the observer, and $\overrightarrow{r_1}$ and $\overrightarrow{\theta_1}$ the base vectors of the spherical coordinates of the radiation pattern of the dipole. This expression depends on several powers of r, and represents the far and near field components of the electric field. As discussed in a previous paper [3], the r^{-2} or r^{-3} terms represent the lamellar part, while the r^{-1} components are linked with the far field and are perpendicular to the propagation direction.
On the other hand, the general expression of a capacitor is given by Eq. 2 :

$$Q = C\ V \rightarrow \int \frac{Q}{4\pi\varepsilon r^2}\ dx = \int \overrightarrow{E}\cdot\ \overrightarrow{dx} \tag{2}$$

in which Q is the charge of the capacitor and x is an axis orthogonal to both armatures of the capacitor.
Moreover, the magnetic far field emitted by an elementary loop can be obtained from Eq. 3 :

$$B(r,\theta) = \mu\pi\frac{I\ S\ \sin\theta}{r\lambda^2} \tag{3}$$

in which I represents the current within the loop, S the surface of the loop and μ the magnetic permeability. In far field, the magnetic field B and the electric field are equivalent. Moreover, the magnetic field is topologically more convenient than the electric field for the representation of the amount of energy exchanged within the field. As can be seen in Fig. 1, the loop generated between the electrostatic field and σE, the conduction current on the main axis on the dipole, is clearly visible.

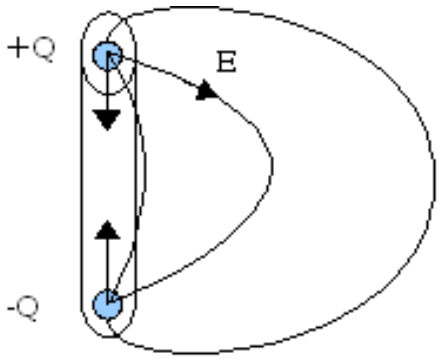

Fig. 1. Conduction current and electric field lines of a dipole

However, due to the number of field lines, the computation of the magnetic flux ϕ requires a clever identification of the trajectory to be used for the closed curvilinear integration of the electric field.

The definition of an associated inductance should then be made possible.
In order to solve this issue, a topological study of the dipole, using Kron's method [5] [1], is used. In this method, loads are associated with the node space level, conduction and displacement currents to the edge space level, and magnetic flux with the mesh space level.
In low frequency (below the first eigenmode), the dipole behaves only like a capacitor, the value of which should remain the same in its equivalent circuit. Then, the inductance value will be deduced from the first resonance value. This capacitance value is the sum of :

- the capacitance of the two disks located at the base of the dipole,
- the capacitance of two plates separated by $2\pi y$ (y is the integration height).

This capacitance can be computed by Eq. 4 :

$$C \approx \varepsilon_0 \left[d \ln\left(\frac{2h}{\Delta}\right) + \pi \frac{d^2}{\Delta} \right] \tag{4}$$

in which d is the radius of one dipole, Δ the base distance between both dipoles, and h the height of the dipole. In this case, with 1-mm diameter, 2-cm high dipoles separated by 3 mm, C is around 12 fF.
Likewise, the capacitance of a two-dipole setup can be computed using the law of capacitance per unit length of a two-wire line, which is illustrated in Eq. 5 :

$$C_2 = \frac{h}{120\, c \ln(\frac{4h}{d})} \tag{5}$$

The next step consists in comparing this capacitance, the loop expression in far field, and Eq. 1. Previous experience as well as several articles have already shown that the method of moments is well suited to the computation of mutual inductance. In this case, the mutual inductance of both coupled dipoles can be computed by Eq. 6 :

$$M_{12} = \frac{\mu}{4\pi} \int_{y_1} \int_{y_2} \frac{\cos(y_1 - y_2)}{\sqrt{D^2 + (y_1 - y_2)^2}}\ dy^2 \tag{6}$$

In the case of 2-cm long dipoles, this mutual inductance is $M_{12} = 3.98 \cdot 10^{-11}$ H, approximated by $3.5 \cdot 10^{-11}$ H. This value is lower than the equivalent self inductance of one dipole ($1/(C{\omega_0}^2) \approx 0.06\ \mu$H), and is actually close to the flux obtained from the average electrostatic field line. As a comparison, the inductance of a loop is equal to (Eq. 7) :

$$L = \frac{1}{2}\ \frac{\pi \mu h}{2} \tag{7}$$

By neglecting the r^{-3} terms in Eq. 1, and seeing that the lamellar component is taken into account in the capacitor interaction, the $\sin\theta$ field intensity (which represents the perpendicular component) can be rewritten as (Eq. 8) :

$$E(r^2) = \jmath \frac{p_0}{4\pi\varepsilon_0 r^2 \lambda} \qquad E(r) = \frac{r}{\lambda}\ \frac{p_0}{4\pi\varepsilon_0 r^2 \lambda} \tag{8}$$

The first term in Eq. 8 represents a capacitance-like expression, while the second one models the far field model linked with the mutual inductance (obtained from the loop interaction in far field). Moreover, the perpendicular evolution of the field can be computed directly from the method of moments and through the magnetic field model, rather than from the electric field. Both terms of the electric dipole in Eq. 8 must be obtained through a magnetic working out, as they are included in the vector potential (the $\overrightarrow{grad}\ \psi$ component is linked with the lamellar part [6]). Then, by adding these terms and using an exponential development, the behavior of the magnetic field B can be expressed in Eq. 9 :

$$M'_{12} = M_{12} e^{-\alpha \frac{r}{\lambda}} \tag{9}$$

3 THE INTERACTION GRAPH

As a result of this study, the interaction graph between both half-wave antennas can then be computed (Fig.2).

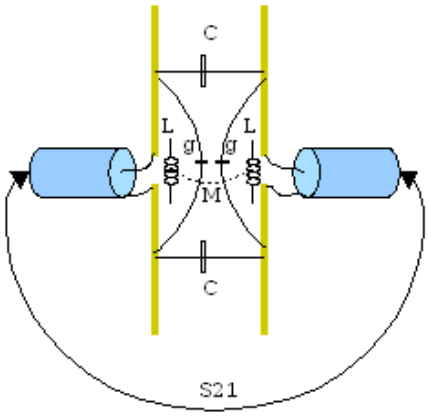

Fig. 2. Interaction between both half-wave antennas

This graph depicts the self inductance of each antenna, the mutual inductance between both antennas, the capacitance of each antenna, and finally the inter-antenna capacitance, thus making it possible to build the corresponding impedance tensor Z in the edge base :

$$Z = \begin{pmatrix} 50 & 0 & 0 & 0 & 0 & 0 \\ 0 & \frac{1}{sg} & 0 & 0 & 0 & 0 \\ 0 & 0 & \frac{1}{sC} & 0 & 0 & 0 \\ 0 & 0 & 0 & \frac{1}{sC} & 0 & 0 \\ 0 & 0 & 0 & 0 & \frac{1}{sg} & 0 \\ 0 & 0 & 0 & 0 & 0 & 50 \end{pmatrix} \tag{10}$$

in which s is the Laplace operator. Likewise, an inductance tensor M can be defined in the mesh base :

$$M = \begin{pmatrix} s\frac{1}{g{\omega_0}^2} & 0 & sM'_{12} \\ 0 & 0 & 0 \\ sM'_{12} & 0 & s\frac{1}{g{\omega_0}^2} \end{pmatrix} \tag{11}$$

This problem can be solved in frequency domain for every distance between both antennas, through Eq. 12, 13 and 14 :

$$Z_{\mu\nu} = L^a_\mu L^b_\nu Z_{ab} + M_{\mu\nu} \tag{12}$$

$$e_\mu = Z_{\mu\nu} I^\nu \tag{13}$$

$$S_{21} = \left| 50 \frac{I^3}{e_1} \right| \tag{14}$$

L is the connectivity matrix providing the relations between the edge base and the mesh base, with a source e in the mesh space. As far as the S_{21} measurement is concerned, the single source is the one injected into the first antenna.

4 EXPERIMENTAL RESULTS

In order to measure the interaction between both antennas, two perfectly identical half-wave antennas are used, which makes inter-antenna distance measurement easier. Each dipole is fastened on a micrometric mechanism allowing an accurate measurement of the distance between the antennas, which is swept between 1 and 19 mm. In order to trigger both near- and far-field interactions, the antennas are fed with a high-frequency (27.5 GHz) generator; consequently, the far-field criterion is met at approximately 3.5 mm ($\frac{\lambda}{\pi}$).
Then, the S_{21} parameter of the interaction is measured and compared with theoretical results obtained with the help of the SCILAB software. These results are presented in Fig. 3.
By fitting the α coefficient in Eq. 9 to 1.1, the discrepancy between measurements theoretical values is lower than 0.6 % in any case, which demonstrates the validity of this study.

5 CONCLUSION

This application (which is the second one using this technique in very near-field interaction) demonstrates the adequation of Kron's method to the simultaneous computation of all kinds of interactions between edges. In the case of near-field EMC, an accurate prediction of the S_{21} parameter, thus an accurate modeling of the injection system, are made possible. In addition to that, this opens to a better understanding of the influence of each kind of interaction.
This study should then be made complete by using 3D electromagnetic software in order to obtain more accurate values of the RLC parameters as well as the mathematical expressions of the interactions involved in this problem.

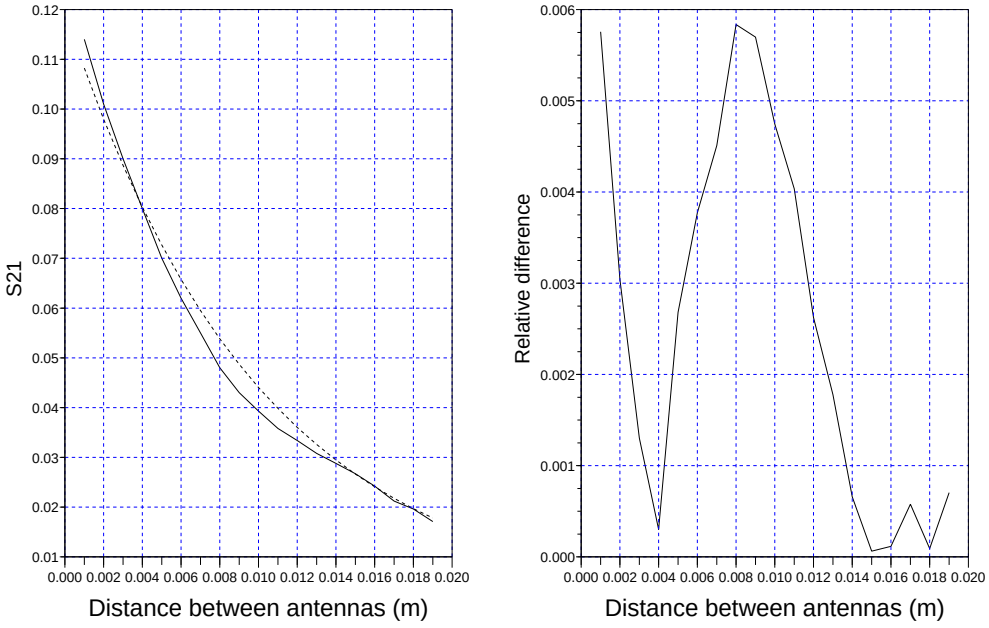

Fig. 3. Left : comparison between measurements (solid) and theoretical values (dotted) for the S_{21} parameter. Right : relative difference between both curves

References

1. O. Maurice. Multiscale, multiphysic analytical method : MKME. *EMC EUROPE 2006, Barcelona*, 2006.
2. A. P. S. Selvadurai. *Partial Differential Equations in Mechanics 2 : the Biharmonic Equation, Poisson's Equation*. Springer, first edition, 2000.
3. O. Maurice. Theoretical discussion on the near and far field concept. *2nd International Conference on Near-Field Charcterization and Imaging (ICONIC 2005), Barcelona*, 2005.
4. P. Lorrain, D. Corson, and F. Lorrain. *Electromagnetic Fields and Waves*. WH Freeman and Co., first edition, 1988.
5. A. Simpson. Kron's method : an algorithm for the eigenvalue analysis of large-scale structural systems. *University of Bristol*, 1972.
6. J. D. Jackson. *Classical Electrodynamics*. Wiley and Sons, third edition, 1998.